

The Influence of 3D Printing Parameters on Pellet-Extruded Hyperelastic Polymers for Cost-Efficient Soft Gripping With Encapsulated Sensors

Andrei-Alexandru Popa and Cristi Teslari

Department of Mechanical and Electrical Engineering, University of Southern Denmark, 6400 Sønderborg, Denmark

ABSTRACT

Recent advances in pellet-extrusion Fused Filament Fabrication (FFF) allow the robust and repeatable 3D printing of materials exhibiting hyperelastic mechanical properties. This study links process parameters such as temperature and printing speed to the mechanical response of hyperelastic structures, as well as to their dimensional accuracy. Three materials of varied hardness, TPU 75 Shore A, TPV 63 Shore A and TPS 30 Shore A, are investigated experimentally for their strength and elasticity, with manufacturing defects further highlighted by analysis under a Scanning Electron Microscope (SEM). The cost-efficient nature of pellet-extrusion FFF lends itself to applications within soft robotic manipulation, with a case study on compliant gripping included in this effort. Leveraging the versatility of FFF towards process pauses and subsequent post-processing, standard sensor components for measuring angle and force are mounted into cavities during and after the print, respectively. The encapsulated sensors validate numerical simulations on the gripper topology, qualifying the force response and object detection capability over 50 use-cycles.

Keywords: 3D printing, Pellet-extruder, Encapsulated sensors, Hyperelastic materials, Soft gripping

INTRODUCTION

Answering an increasingly demanding market for small and medium volume production of complex parts, additive manufacturing (AM) – otherwise known as 3D printing – has been successfully employed to create custom prototypes for decades (Godec et al., 2022). Among the seven recognized 3D printing technologies according to ISO/ASTM taxonomy (ISO/ASTM52900, 2021). Fused Filament Fabrication (FFF), a vastly popular form of thermoplastic extrusion, stands out as cost-efficient means of rapid prototyping (Ferretti et al., 2022) using feedstock in both filament and granulate form. Known as Fused Granulate Modeling (FGM) or pellet thermoplastic extrusion, the latter variation presents several advantages over the former, including a wider range of materials, faster print rates due to increased nozzle sizes, larger build envelopes and reduced feedstock cost (Shaik et al., 2021). Figure 1 (Martin et al., 2022) depicts the functioning principle.

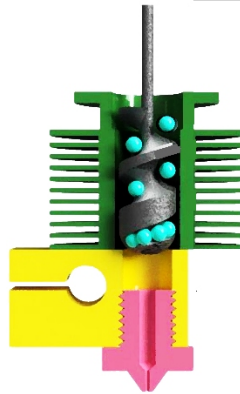


Figure 1: FGM extruder components (granules in cyan).

Heavily dependent on process parameters, the tailoring of mechanical response and overall properties of 3D printed components implies a thorough understanding of and synergy between the manufacturing hardware, the desired material and the printing strategy for any given application (Godec et al., 2022). Still, with its virtually limitless design space, AM has established itself as a transformative fabrication method for a range of industries spanning across aerospace, wearables and biomedicine, all the way to electronic interfaces (Carradero Santiago et al., 2020) to robotic grippers and actuators (Georgopoulou & Clemens, 2022).

Soft pneumatic actuators are usually fabricated with a molding process by 3D printed molds into which silicone rubbers are cast and consolidated. These components offer durability, biocompatibility, and high deformation levels at low pressures. The molding process, however, is time-consuming and requires significant manual assembly, which can create issues with weak seams, repeatability, and accuracy (Walker et al., 2019). In addition, complex geometries often require multistage casts using techniques such as overmolding, along with the addition of strain limiting layers or fiber reinforcements (Hainsworth et al., 2020). The use of direct additive manufacturing for soft robotic fabrication takes full advantage of the available 3D-printing technologies, such as reduced manual tasks and the ability to fabricate very complex geometries, intricate circuits, and multicomponent designs in an all-in-one manufacturing setup (Walker et al., 2019).

Sensing elements have been integrated into AM substrates in various forms (Popa et al., 2019; Popa et al., 2021). In soft robotics, they are linked to monitoring the position and physical characteristics of effectors, enabling their accurate and agile control.

This paper seeks to fill in the research gap on the effect of various printing parameters and material selection in the cost-effective design and manufacturing of soft grippers by FGM. While other efforts within 3D printed soft gripping tend to focus either on application specific designs and their control strategies (Tawk et al., 2022), or on the behaviour of niche materials with previously uncharacterized response (Singamneni et al., 2021; Dezaki, et al., 2023), the current work offers comparative insight into a range of

three commercially available hyperelastic materials (TPU 75 Shore A, TPV 63 Shore A and TPS 30 Shore A). The study is completed a soft gripping use case.

METHOD

Qualifying the influence of several printing parameters on the mechanical response and general quality of the manufactured components is vital towards subsequent design and material selection for soft gripping. This study analyses the impact of nozzle temperature, printing speed, infill pattern and perimeter overlap, flow rate, and layer height on the properties of 3D printed hyperelastic samples, as follows.

By prototyping test cubes of side length 10mm and using the Archimedes density method, the *porosity* of 165 samples was linked to various printing parameters. *Tensile strength* was investigated for 195 samples, by creating dogbone shaped specimens according to ASTM D412 (Figure 2), subject to uniaxial tensile loading at a rate of 50 mm/min on a Lloyd LD30 machine equipped with a 1 kN load cell.

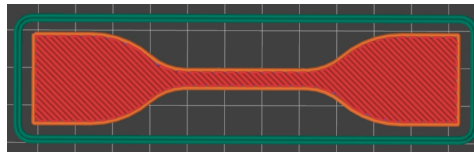


Figure 2: Tensile “dog bone” specimen.

Extracting the parameter sets that yielded the highest UTS for each material, the *dimensional accuracy* of 15 cuboid samples of base 30 mm by 30 mm and height 15 mm was obtained using Equation 1 (Xu et al., 2023).

$$\text{Printing Accuracy(\%)} = \frac{\left(1 - \frac{|H_z - H_d|}{H_z}\right) + \left(1 - \frac{|H_z - H_d|}{H_z}\right) + \left(1 - \frac{|L_s - L_{BE}|}{L_s}\right) + \left(1 - \frac{|L_s - L_{BCl}|}{L_s}\right) + \left(1 - \frac{|W_s - W_{BE}|}{W_s}\right) + \left(1 - \frac{|W_s - W_{BCl}|}{W_s}\right)}{6}$$

Equation 1 - Printing accuracy measured between set distances, edge and centres.

To observe the *microstructure* of the 3D printed samples, a Hitachi S–4800 scanning electron microscope (SEM) was used.

The choice of process parameter values to be included in this study is the product of literature review (Wang et al., 2020; Hou et al., 2020; Ju et al., 2022) together with manufacturer recommendations (Direct3D, 2024) for each specific granulate type. Specifically, temperatures of 190–210 °C are chosen for TPU, 170–190 °C for TPS and 220–240 °C for TPV. Printing speeds vary between 20–40 mm/s for all materials, with a similarly shared layer height of 0.2–0.4 mm. Perimeter overlaps are taken between 50–100%, while flow rates are controlled by the extrusion multiplier. TPV required the highest multiplication, 600–650%, while TPS was tested between 150–170% and TPU within 90%–110%.

In the context of low-cost soft gripper fabrication, robustness to process parameter changes and general ease of 3D printing – linked to fewer

costly printing failures – constitute the criteria of selection of the material to be employed in a case study involving the design, simulation, fabrication and testing of hyperelastic gripping topologies. For functionality monitoring and characterization, two types of sensors, bending and force sensors, are specifically implemented into a mechanically actuated 3D printed soft gripper. Soft bending actuator deformation is often tracked and monitored using flexure or bend sensors. These sensors are intended to identify and quantify the actuator's degree of flexure or bending, offering insightful information about the actuator's form and motion. The integration of these 3D printed fingers with electronics have three possible manufacturing strategies: (a) during fabrication with process interruptions, (b) after fabrication with the insertion of components into structural cavities, or (c) after the fabrication with components interposed between two printed structures that are subsequently polymer overmolded together (Carradero Santiago et al., 2020). Consequently, the first two strategies were chosen individually for the selected sensors.

RESULTS AND DISCUSSION

The examined samples were all printed on the same machine, a modified Anycubic Kobra Max with an FGM module. The printing direction and orientation of parts was identical across all samples.

Density

The porosity of structures has a dominant effect on their mechanical behaviour. By measuring the density of small samples, this effect can be tuned by porosity-influencing process parameters. Figure 4 contains the results for all three materials obtained by the Archimedes density method.

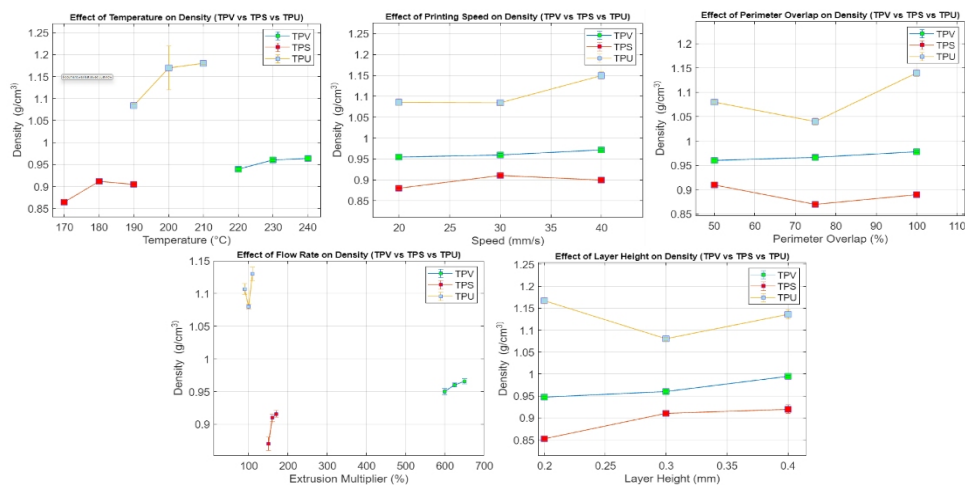


Figure 3: The effect of printing parameters on density for TPU, TPS and TPV.

For TPV, higher temperatures and elevated flow rates, together with increased printing speeds and larger layer heights positively impact the density. Decreasing the layer height of TPS prints to 30 mm/s leads to a significant decrease in porosity (5–7%), although further decreasing does not induce a positive effect.

Similarly, the optimum temperature stands out mid-range. Porosity is lowered, however, by an increase in perimeter overlap, layer height and flow rate. Increasing the speed and temperature for TPU are linked to density increase. The impact of, for instance, perimeter overlap and layer height on density suggests a more complex interplay in optimizing its printing parameters.

Tensile Strength

The influence of printing parameters on the tensile strength of printed components is crucial to their design against load. As Figure 4 suggests, there are again significant variations in TPU dependent on process parameters, with TPS and, particularly, TPV revealing more robust response across the range of changes.

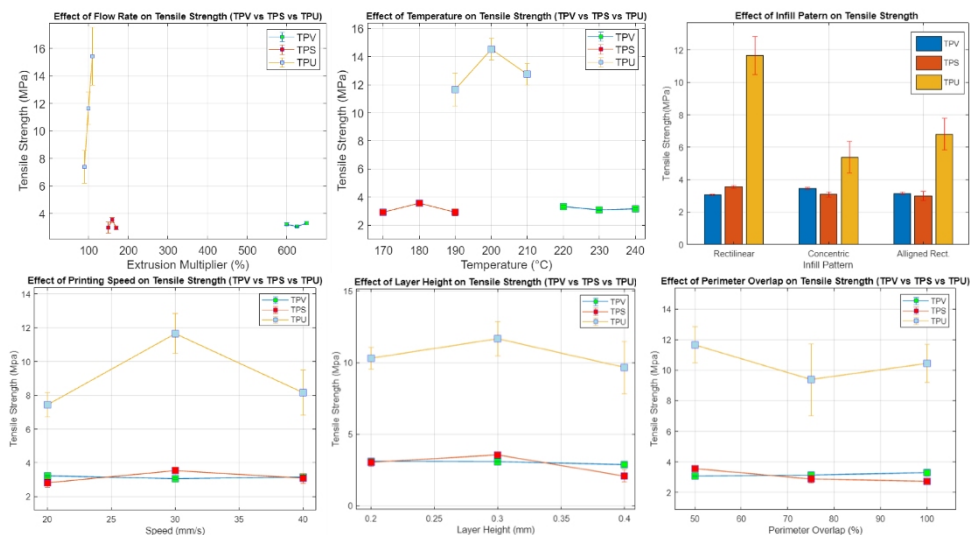


Figure 4: The effect of printing parameters on UTS for TPU, TPS and TPV.

For the latter, the highest tensile strength is linked to concentric infill patterns and a decrease in temperature to 220 °C, along with increases in flow rate (650%) and perimeter overlap (100%). In the case of TPS, the rectilinear infill pattern demonstrated the highest strength, while the other variations yielded nearly identical results. Simultaneously, raising the flow rate from 150% to 160% correlates to a 16% increase in strength, yet a subsequent increase to 170% leads to a substantial decline. The optimal printing speed was found as 30 mm/s, with deviations generating inferior results in UTS. Similarly to TPS, TPU also witnesses a positive impact on UTS by increasing the extrusion temperature, with a notable 19.75% increase when transitioning from 190 °C to 200 °C. The most significant increase is noticed linked to

raising the flow rate from 90% to 110% - specifically 47.9% as an average across samples.

These results produce a set of parameters that generate the highest UTS for all materials, as found in Table 1.

Table 1. Printing parameters used in subsequent testing.

Material	Temp (°C)	Flow Rate	Speed (mm/s)	Layer height (mm)	Perimeter Overlap
TPV 63A	220	650%	20	0.3	100%
TPS 30A	180	160%	30	0.3	50%
TPU 75A	190	100%	30	0.3	50%

Printing Accuracy

Cuboids were produced to investigate the accuracy, at an infill of 30%. Figure 5 shows that TPV had not only the highest accuracy in printing, but also the smallest deviation between samples.

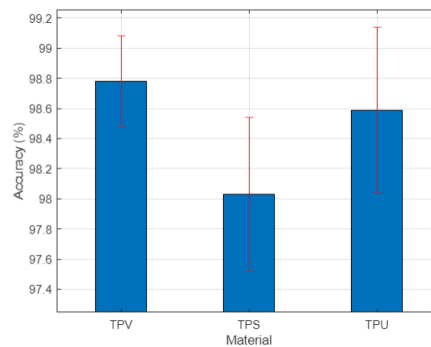


Figure 5: Accuracy chart.

Microstructure (SEM Analysis)

The same samples are used to conduct an SEM analysis, after sputter coating with a 10nm thick layer of Platinum Paladium. Figure 6 reveals TPU results, while Figure 7 and Figure 8 contain information on TPS and TPV, respectively.

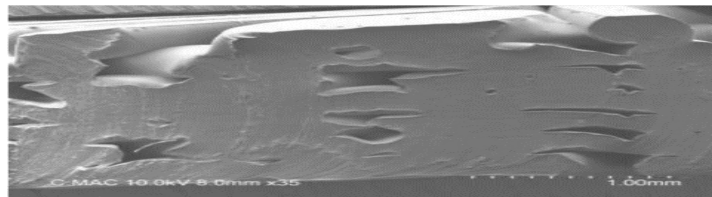


Figure 6: Cross section of TPU at 1mm and 50 μ m scale.

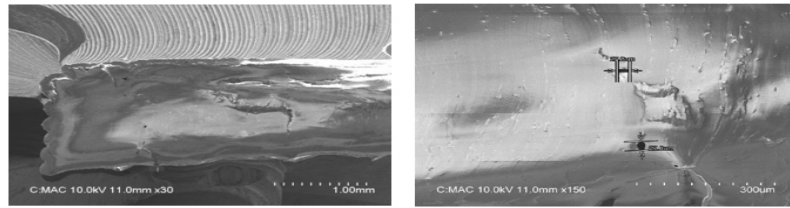


Figure 7: Cross section of TPS at 1mm and 300 μ m scale.

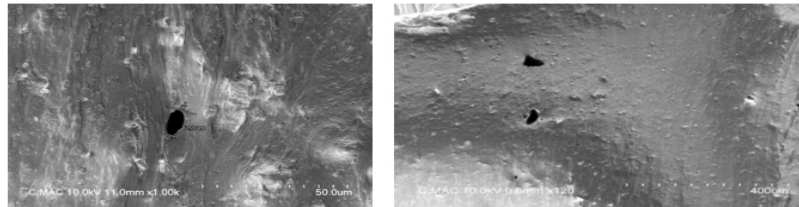


Figure 8: Cross section of TPV at 50 μ m and 400 μ m scale.

TPU exhibits the highest abundance of defects, particularly substantial voids at a scale of 1 mm, together with those ranging from 10 μ m to 32 μ m. TPS and TPV reveal fewer and smaller voids, suggesting superior bonding. The selection of materials based on robustness to change, consistency between samples and overall printability, altogether in the scope of cost-efficient 3D printing of soft grippers, would support either TPS or TPV as the material of choice, with a slight edge for the latter due to its empirically observed quality against oozing from the extruder. Moreover, research on TPV for soft grippers is not extensive, rendering it of particular interest for the below case study.

Mechanically Actuated Compliant Gripper (MACG)

A compliant gripper design is simulated in Ansys and manufactured in TPV. Figure 9 illustrates the correlation between the numerics and the real-life behaviour of the structure.

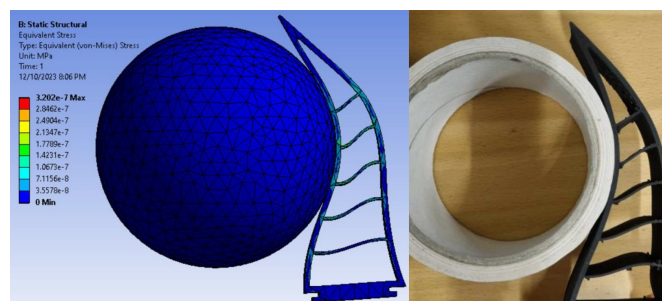


Figure 9: Simulation and real deformation of compliant gripper against a curved surface.

A force sensor is inserted into a cavity while pausing the 3D print, with the process resuming afterwards. The advantage of using this technique is the absence of post processing. Figure 10 shows the concept, together with that of embedding the flex sensor post-print. The possibility of using both methods in the same component highlights the robustness of the concept.

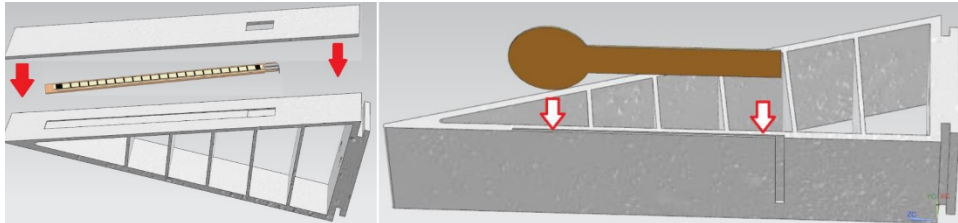


Figure 10: Flex (left) and force (right) sensor integration within 3D printed substrate.

A gripping device is constructed using three 3D printed grippers actuated by a motor and a lead screw, such that objects of various sizes can be picked up and held (Figure 11). To test robustness, the assembly is tested on a spherical object, yielding the results of Figure 12.

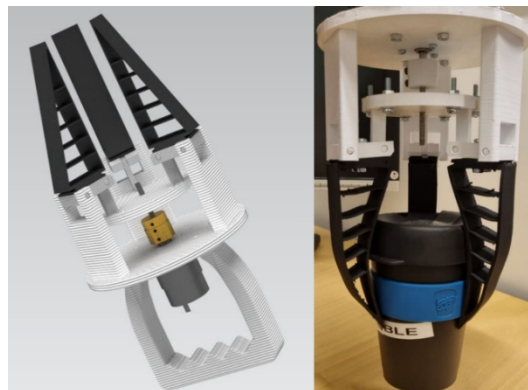


Figure 11: Compliant gripper design (left) and prototype (right).

It is obvious that over 50 cycles, the force response fluctuates, albeit not at the sacrifice of functionality. The assembly of the device, rather, is the cause of the jagged behaviour, with mechanical improvements that are not central to this effort needed. The angle graph from the flexure sensor, however, exhibits promising continuity.

The device can be of medical use for humans with motor deprivation, as the compliant nature of the grippers allow for imperfect and oscillating motion in its handling, while not compromising the structure of the target object due to force and angle monitoring. These aspects can be improved by a feedback system which can be tuned for different types of object stiffness.

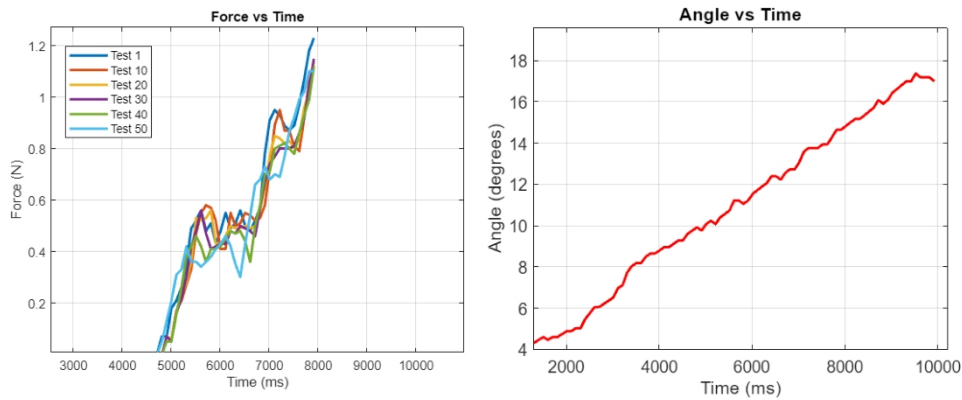


Figure 12: Force and angle response of gripper mechanism.

CONCLUSION

This research successfully established correlations between five printing parameters and the mechanical properties of three hyperelastic materials used in additive manufacturing. The investigation, covering density and tensile strength tests, revealed some complex relationships crucial for defining a reliable baseline of the materials' physical characteristics, ultimately improving printing quality. With respect to variations in process parameters, TPV stands out as the most robust material compared to TPS and TPU, making it an interesting, safe choice for cost-efficient rapid prototyping of soft grippers. By encapsulating sensors during and post-print, intelligent grippers with embedded sensing can be developed, broadening prototyping possibilities within object detection and manipulation.

The findings of the study are not restricted to robotics, and future research may explore the use of the investigated hyper-elastic materials in applications within vibration damping, shock absorption or human wearables.

ACKNOWLEDGMENT

The authors would like to acknowledge the Fabrikant Mads Clausen Foundation for funding the acquisition of the 3D printing equipment used in this study.

REFERENCES

- Carradero Santiago, C. et al., 2020. 3D Printed Elastomeric Lattices With Embedded Deformation Sensing. *IEEE Access*, Volume 8, pp. 41394–41402.
- Czepiel, M., Bańkosz, M. & Sobczak-Kupiec, A., 2023. Advanced Injection Molding Methods: Review. *Materials (Basel)*, Volume 17.
- Dezaki, M. L. et al., 2023. Soft pneumatic actuators with integrated resistive sensors enabled by multi-material 3D printing. *The International Journal of Advanced Manufacturing Technology*, Volume 128, pp. 4207–4221.
- Direct3D, 2024. *Direct3D*. [Online]. Available at: <https://www.direct3d.it/> [Accessed 30 January 2024].

- Ferretti, P. et al., 2022. Production readiness assessment of low cost, multi-material, polymeric 3D moulds. *Heliyon*, 8(10).
- Georgopoulou, A. & Clemens, F., 2022. Pellet-based fused deposition modeling for the development of soft compliant robotic grippers with integrated sensing elements. *Flexible and Printed Electronics*, Volume 7.
- Godec, D. et al., 2022. *A Guide to Additive Manufacturing*. First ed. Cham, CH: Springer.
- Gohn, A. M. et al., 2022. Mold inserts for injection molding prototype applications fabricated via material extrusion additive manufacturing. *Additive Manufacturing*, Vol. 51.
- Habrman, M. et al., 2023. Injection Moulding into 3D-Printed Plastic Inserts Produced Using the Multi Jet Fusion Method. *Materials*, Volume 16.
- Hainsworth, T., Smith, L., Alexander, S. & MacCurdy, R., 2020. A Fabrication Free, 3D Printed, Multi-Material, Self-Sensing Soft Actuator. *IEEE Robotics and Automation Letters*, 5(3), pp. 4118–4125.
- Hou, J. et al., 2020. Fabricating 3D printable BIIR/PP TPV via masterbatch and interfacial compatibilization. *Composites Part B*, Volume 199.
- Hyatt, J. & Hyatt, J., 1872. *Improvement in Process and Apparatus for Manufacturing Pyroxyline*. United States of America, Patent No. US133229.
- ISO/ASTM52900, 2021. *Additive Manufacturing-General Principles-Terminology*.
- Ju, Q. et al., 2022. Thermoplastic starch based blends as a highly renewable filament for fused deposition modeling 3D printing. *International Journal of Biological Macromolecules*, Volume 219.
- Kanishka, K. & Acherjee, B., 2023. Revolutionizing manufacturing: A comprehensive overview of additive manufacturing processes, materials, developments and challenges. *Journal of Manufacturing Processes*, Volume 107.
- Kazmer, D. et al., 2023. Strategic cost and sustainability analyses of injection molding and material extrusion additive manufacturing. *Polymer Engineering and Science*, Volume 63, pp. 943–958.
- Martin, V. et al., 2022. Low cost 3d printing of metals using filled polymer pellets. *HardwareX*, Volume 11.
- Popa, A.-A., Drimus, A., MacDonald, E. & Duggen, L., 2021. A Conformal, Optimized 3D Printed Kneepad With Deformation Sensing. *IEEE Access*, Volume 9, pp. 126873–126881.
- Popa, A.-A., Mai, C., Duggen, L. & Jouffroy, J., 2018. *Towards Printing Mechatronics: Considerations for 3D-printed conductive coupling*. Auckland, NZ, IEEE.
- Popa, A.-A. et al., 2019. *3D Printed Hybrid Flexible Electronics with Direct Light Synthesis*. s.l., Springer.
- Shaik, Y. P., Schuster, J. & Shaik, A., 2021. A Scientific Review on Various Pellet Extruders Used In 3D Printing FDM Processes. *Open Access Library Journal* 8, Volume 8.
- Shapley, D., 1978. Industry Takes to “Potting” Its Products for Market. *Science*, 24 November, Volume 202, pp. 848–849.
- Singamneni, S. et al., 2021. Direct extrusion 3D printing for a softer PLA-based bio-polymer composite in pellet form. *Journal of Materials Research and Technology*, Volume 15, pp. 936–949.
- Tawk, C., Sariyildiz, E. & Alici, G., 2022. Force Control of a 3D Printed Soft Gripper with Built-In Pneumatic Touch Sensing Chambers. *Soft Robotics*, 9(5).

-
- Walker, S., Yirmibeşoğlu, O., Daalkhaijav, U. & Mengüç, Y., 2019. Additive manufacturing of soft robots. *Robotic Systems and Autonomous Platforms*, pp. 335–359.
- Wang, J. et al., 2020. Research of TPU Materials for 3D Printing Aiming at Non-Pneumatic Tires by FDM Method. *Polymers*, Volume 12.
- White, J., 1990. *Principles of Polymer Engineering Rheology*. New York: Wiley.
- Xu, M. et al., 2023. Exploring the mechanism of variation in 3D printing accuracy of cassava starch gels during freezing process. *Food Hydrocolloids*, Volume 140.